Biosensors and Bioelectronics xxx (2010) xxx–xxx

Contents lists available at ScienceDirect

Biosensors and Bioelectronics

journal homepage: www.elsevier.com/locate/bios

Fast cholesterol detection using flow injection microfluidic device with functionalized carbon nanotubes based electrochemical sensor

A. Wisitsoraat*, P. Sritongkham, C. Karuwan, D. Phokharatkul, T. Maturos, A. Tuantranont*

Nanoelectronics and MEMS Laboratory, National Electronics and Computer Technology Center, 112 Pahol Yothin Rd., Pathumthani 12120, Thailand

ARTICLE INFO

Article history:
Received 14 April 2010
Received in revised form 22 July 2010
Accepted 26 July 2010
Available online xxx

Keywords:
Flow injection
Microfluidic device
Carbon nanotube
Cholesterol
Enzyme based biosensor
In-channel electrochemical detection
Lab-on-a-chip

ABSTRACT

This work reports a new cholesterol detection scheme using functionalized carbon nanotube (CNT) electrode in a polydimethylsiloxane/glass based flow injection microfluidic chip. CNTs working, silver reference and platinum counter electrode layers were fabricated on the chip by sputtering and low temperature chemical vapor deposition methods. Cholesterol oxidase prepared in polyvinyl alcohol solution was immobilized on CNTs by in-channel flow technique. Cholesterol analysis based on flow injection chronoamperometric measurement was performed in 150-μm-wide and 150-μm-deep microchannels. Fast and sensitive real-time detection was achieved with high throughput of more than 60 samples per hour and small sample volume of 15 μl. The cholesterol sensor had a linear detection range between 50 and 400 mg/dl. In addition, low cross-sensitivities toward glucose, ascorbic acid, acetaminophen and uric acid were confirmed. The proposed system is promising for clinical diagnostics of cholesterol with high speed real-time detection capability, very low sample consumption, high sensitivity, low interference and good stability.

1. Introduction

Microfluidic system is a potential platform for biochemical processing and analysis with numerous advantages including low sample/reagent consumption, high sample throughput and total analysis capability (Becker and Locascio, 2002; Rwyes et al., 2002). Recently, plastic/glass based microfluidic platforms have been widely employed in various microfluidic applications. Polymethylmethacrylate (PMMA) (Ford et al., 1998) and polydimethylsiloxane (PDMS) (McDonald et al., 2000) are among the most popular plastic materials for biochemical microsystems due to low cost, ease of fabrication, high chemical/mechanical stability and bio-compatibility (Schoning et al., 2005).

Integration of efficient sensors on microfluidic chips has been one of the most important tasks for the development of micro-total analysis system. Optical detection schemes such as fluorescence, surface plasmon resonance and ultraviolet spectrophotometer have been widely used in biochemical analyses. However, cost and complexity make them impractical for microfluidic platforms. Electrochemical technique is another well-known biochemical detection method, which offers high performance detection as well as compatibility with microsystems (Lin et al., 2008). Recently, electrochemical detection has been embedded in microfluidic systems based on end-channel (Castano-Alvarez et al., 2006; Pozo-Ayuso et al., 2008) and in-channel (Liao et al., 2007; Dossi et al., 2007) detection schemes using different electrode materials, including gold, platinum and carbon paste. Nevertheless, conventional electrochemical electrodes are not fast and sensitive enough for micro-total analysis applications, which involve small analyte volume and short detection time. Therefore, the integration of novel sensing materials in microfluidic platform has been an important research focus for the development of advanced bio/chemical analysis systems.

Cholesterol is an essential lipid with several biological functions in organisms. The determination of cholesterol level in food and blood has been increasingly important for clinical analysis/diagnosis because of reported alarming rise in the rate of clinical disorders due to abnormal levels of blood cholesterol. Thus, there has been continuous effort to develop rapid and sensitive cholesterol sensors and systems (Arya et al., 2008; Li et al., 2010). Electrochemical cholesterol sensors utilizing various matrix and electrode materials with different enzyme immobilization methods have been widely investigated (Vidal et al., 2001; Brahim et al., 2002; Li et al., 2003; Guo et al., 2004; Qiaocui et al., 2005; Yang et al., 2006; Arya et al., 2007; Ansari et al., 2008, 2009; Umar et al., 2009; Solanki et al., 2009; Kaushik et al., 2010).

* Corresponding authors. Tel.: +66 2 564 6900; fax: +66 2 564 6771.
E-mail addresses: anurat.wisitsoraat@nectec.or.th (A. Wisitsoraat), adisorn.tuantranont@nectec.or.th (A. Tuantranont).

0956-5663/$ – see front matter © 2010 Elsevier B.V. All rights reserved.
doi:10.1016/j.bios.2010.07.101

The integration of cholesterol sensor in microfluidic platform will offer instant blood cholesterol determination capability since complete processing from serum extraction to detection can be continuously performed on one chip. Recently, cholesterol sensors based on gold nanowires prepared by electroplating through anodized alumina template were integrated in a microfluidic platform by dielectrophoresis coating (Aravamudhan et al., 2007). However, the reported gold nanowires sensor only provided a factor of two sensitivity improvement relative to a thin gold film electrode because the method produced relatively large-size gold nanowires. In addition, the detection was conducted using square wave voltammetry rather than real-time flow injection analysis due possibly to weak bonding between nanowires and gold contact. Therefore, more efficient nanostructure materials and better integration method should be employed to yield fast and sensitive flow injection based cholesterol detection.

Carbon nanotubes (CNTs) are promising for electrochemical sensing due to huge surface area, high electrical conductivity and excellent electron transfer rate. CNTs have been widely used as sensors in various electroanalysis and bio-sensing applications (Huang et al., 2003; Shahrokhian and Zare-Mehrjardi, 2007; Kirgoz et al., 2007). In addition, CNTs are reported to have excellent cholesterol sensing performance with high sensitivity, low detection potential and fast response (Guo et al., 2004; Li et al., 2005; Roy et al., 2006; Yang et al., 2006; Solanki et al., 2009; Wisitsoraat et al., 2009). Recently, there have been reports on the use of screen printed CNT paste electrodes on microfluidic chips for chemical and biological analyses (Panini et al., 2008; Crevillen et al., 2009; Dossi et al., 2009). Moreover, unmodified CNTs have been directly integrated on glass based microfluidic chip for rapid salbutamol sensing (Karuwan et al., 2009). However, there has been no report on the use of CNTs integrated on a microfluidic chip for real-time cholesterol detection.

In this work, a new cholesterol sensing scheme is developed based on in-channel amperometric flow injection analysis utilizing carbon nanotube (CNT) electrode integrated on a PDMS/glass microfluidic chip. The uniqueness of this approach is the direct growth of CNT electrode on a glass based chip by a low temperature chemical vapor deposition (CVD) process. The on-chip CNTs growth approach offers considerably higher density and better aligned CNT structure with much stronger substrate adhesion than other reported methods including CNT paste printing or dielectrophoresis deposition. It will be an ideal platform for micro-flow injection based biosensors. For cholesterol detection, cholesterol oxidase is immobilized on CNTs by simple but effective in-channel enzyme entrapment using polyvinyl alcohol matrix.

2. Experimental

2.1. Chemicals and reagents

All of chemicals used in this work were analytical grade reagent. Cholesterol (CHO), cholesterol oxidase (ChOx, Pseudomonas fluorescens 25 U/mg), potassium hexacyanoferrate, glucose, acetaminophen, ascorbic acid and Triton X-100 were purchased from Sigma–Aldrich. Phosphate buffer saline (PBS) solution was acquired from Fluka (USA). 98–99% hydrolyzed polyvinyl alcohol (PVA) was obtained from Alfa Aesor (USA). Glass substrates were purchased from Sperior (Germany). PDMS were purchased from Dow Chemical (USA) and photoresist (SU-8 2100) was procured from Micro Chem (USA).

2.2. Apparatus

A potentiostat, μ-autolab Type III (Metrohm, Switzerland) was utilized for all amperometric studies. Spin coater (Laurell technologies Corp, model WS-400A-6NPP) was used for spin coating of photoresist for mold fabrication. MJB4 mask aligner (SUSS microtec, Germany) was the tool for standard UV-lithography process. Oxygen plasma system (Harrick scientific Corp., model PDC-32G) was employed for the treatment of PDMS and glass surfaces. Hitachi S4700 field emission scanning electron microscope (SEM) was used to characterize the morphology of CNT electrodes. Perkin Elmer System—Spectrum Spotlight 300 Fourier transform infrared (FTIR) spectroscopic microscope operated in Specular reflection mode was utilized to identify organic compositions on modified CNT electrodes.

2.3. Fabrication of microfluidic device

The fabrication process consisted of three main tasks. Firstly, PDMS chip containing microchannel was made by micromolding and casting processes. Secondly, three-electrode system was formed on a glass substrate by sputtering and chemical vapor deposition (CVD) processes. Lastly, PDMS and glass chips were bonded using oxygen plasma treatment.

For the fabrication of a PDMS chip, SU8 micromold was fabricated by standard photolithography. SU-8 photoresist was spin-coated on a Si substrate and then soft baked to remove sol-

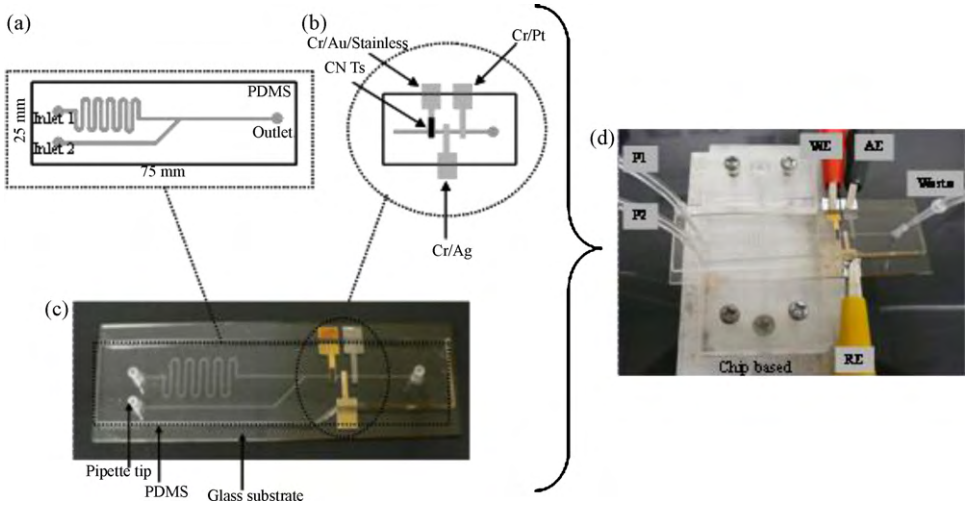

Fig. 1. Diagram and photographs of the microchip with in-channel carbon nanotubes based amperometric detector.

Please cite this article in press as: Wisitsoraat, A., et al., Biosens. Bioelectron. (2010), doi:10.1016/j.bios.2010.07.101

vent in the layer. Next, UV-lithography was performed using MJB4 mask aligner to obtain photoresist patterns on the substrate. The photoresist was then post-baked in order to selectively cross-link the exposed portion of photoresist. Next, the photoresist was developed and cleaned with isopropyl alcohol and deionized water. The microfluidic chip was designed to have two inlets and one outlet as shown in Fig. 1(a). For two inlets, one was used for buffer carrier stream or PVA functionalization and the other was used for injection of analyte or enzyme immobilization. The microchannel was 150 μm deep and 150 μm wide.

In the second part, working (CNTs), auxiliary (Pt) and reference (Ag) electrodes were designed as straight stripes across microchannel and located opposite to the outlet of microchannel as shown in Fig. 1(b). Pt and Ag electrodes were 200 μm wide and 300 nm thick platinum and silver layers each supported by 50 nm Cr adhesive layers while the CNT electrode was formed on a 200 μm wide and 300 nm thick Au contact layer with a 50 nm thick Cr binding layer. For CNT's growth, 10 nm thick aluminum oxide and 5 nm thick stainless steel layers were successively deposited at the end of Au stripe across the microchannel. All layers were deposited and patterned by sputtering through electroplated Ni shadow masks. Ni shadow masks were made by photolithographic patterning and Ni electroplating processes. The aluminum oxide layer was deposited by reactive sputtering at a pressure of 3×10^{-3} mbar of 1:5 Ar/O_2 gas mixtures while other metallic layers were deposited in Ar gas at the same pressure.

CNTs were then grown by a low temperature CVD process (Wisitsoraat et al., 2006). The CVD process was used because of its low cost and ability to produce high quality CNT structure. The prepared glass substrate with electrode and catalyst layers was placed at the gas exit end of a horizontal tube furnace. The furnace was heated up to a center temperature of 700 °C under hydrogen flow of 1500 sccm at atmospheric pressure. It should be noted that high activation center temperature of 700 °C and low substrate temperature of 550 °C were specifically designed to grow CNTs on a glass substrate with melting point of 600 °C. CNTs were grown by acetylene addition with acetylene to hydrogen flow ratio of 1:4 for 1.5 min. In the course of CNT growth, in situ water-assisted etching was employed to remove undesired amorphous carbon formation from random acetylene decomposition (Wisitsoraat et al., 2008). In water etching process, 300 ppm of water vapor was introduced by water bubbling through Ar gas for 3 min while acetylene gas was turned off. CNT's growth and water-assisted etching were repeatedly performed for five cycles.

In the last part, the PDMS and glass chip were treated in 35-W radio-frequency oxygen plasma for 30 s. They were then immediately aligned and attached after oxygen plasma treatment as shown in Fig. 1(c). The inlets and outlet of microchannels were drilled and connected to micro-tubing via pipette tips, which were sealed to PDMS holes by physical attachment as shown in Fig. 1(d). The inlet tubes were connected to syringe pumps and the outlet tube was directed to a reservoir. Finally, the whole apparatus was mounted on an aluminum fixture and electrodes were wired to Potentiostat.

2.4. Enzyme immobilization

Before enzyme immobilization, CNT electrode was functionalized by flow based coating of an aqueous solution of PVA. The polymer solution was prepared by dissolving PVA in deionized water (18.2 MΩ) at a concentration of 0.1% (w/v) and heated to 90 °C for 1 h with constant stirring. The PVA solution was delivered into the channel to CNT electrode using a syringe pump at a flow rate of 10 μl/min for 20 min. Coating with PVA resulted in a highly hydrophilic surface and PVA introduced OH– group on surface, which greatly helped immobilization of various chemical and biological species (Roy et al., 2006).

For enzyme immobilization, cholesterol oxidase solution was prepared by dissolving calculated amount of cholesterol oxidase (25 U/mg) and potassium hexacyanoferrate (redox mediator) in 3 ml PVA solution (0.1% w/v in 0.2 M phosphate buffer, pH 7.0). The cholesterol enzyme concentration was varied between 25 U/ml and 100 U/ml. The enzyme solution was then delivered to CNT electrode using a syringe pump at a flow rate of 10 μl/min for 20 min and PBS buffer stream was flowed to rinse of excess enzyme on CNT electrode. After immobilization, the sensor chip was stored in a refrigerator for 24 h before use.

2.5. Microfluidic flow injection procedure

The 500 mg/dl stock cholesterol solution was prepared by adding required amount of cholesterol to 5 ml of Triton X-100 and then heated up to 90 °C for some time until cholesterol was completely melted. 45 ml of PBS (pH 7.0) solution was then added to Triton X and cholesterol mixture. For interference characterization, the stock solutions of glucose, acetaminophen and ascorbic acid were prepared in deionized water at concentration of 100, 2, 1 and 5 mg/dl, respectively. Before use, all solutions were filtered through 0.2 μm cellulose acetate membrane to prevent clogging in microchannels.

Before flow sensing experiments, microchannels were treated with deionized water for 10 min. PBS running buffer was then continuously delivered into the channel at a flow rate of 40 μl/min. CHO analysis based on flow injection chronoamperometric detection mode was then performed. CHO pulses were injected into the buffer stream and electrochemical current was continuously monitored at a fixed detection potential ranging from +0.3 to +0.6 V vs. Ag reference electrode. Sample injections were performed after stabilization of baseline buffer signal. The current response and throughput were then characterized as a function of injection volume. In addition, the current response was optimized as a function of pH of buffer, enzyme concentration and ambient temperature. The pH of PBS buffer was adjusted by small addition of HCl or NaOH and ambient temperature was controlled by laboratory's air conditioning and heating system. After cholesterol detection, interference responses toward glucose, acetaminophen, uric acid and ascorbic acid were measured at their nominal concentrations.

3. Results and discussion

3.1. On-chip CNT electrode

The surface morphology of on-chip CNT electrode was examined using SEM. Typical top view and cross-sectional view SEM images of CNTs after PVA–enzyme immobilization are shown in Fig. 2(a) and (b), respectively. From Fig. 2(a), it can be seen that CNTs are coated by polymer–enzyme nanoparticles on CNT surface. The size of PVA–enzyme nanoparticles is in the range between 20 and 100 nm. From Fig. 2(b), the nominal diameter of CNTs is ~20 nm and the line density of CNTs is ~40 nanotubes per micron. Thus, the total number of CNTs over 200 μm × 150 μm electrode can be estimated to be $\sim 4.8 \times 10^7$ and approximately 60% of them are coated with PVA–enzyme nanoparticles as seen in Fig. 2(a). The high density CNT integration will be difficult to achieve by other methods including CNT paste printing or dielectrophoresis coating.

The binding of PVA and enzymes on CNT surface was characterized by FTIR spectroscopy. The FTIR spectrum of immobilized CNT electrode is shown in Fig. 3. The observed functional groups indicate successful cholesterol enzyme immobilization. OH band (3200–3570 cm^{-1}), C=O bending peak (~1700 cm^{-1}) and C–O stretching peak (~1110 cm^{-1}) are contributed by PVA (Mansur et

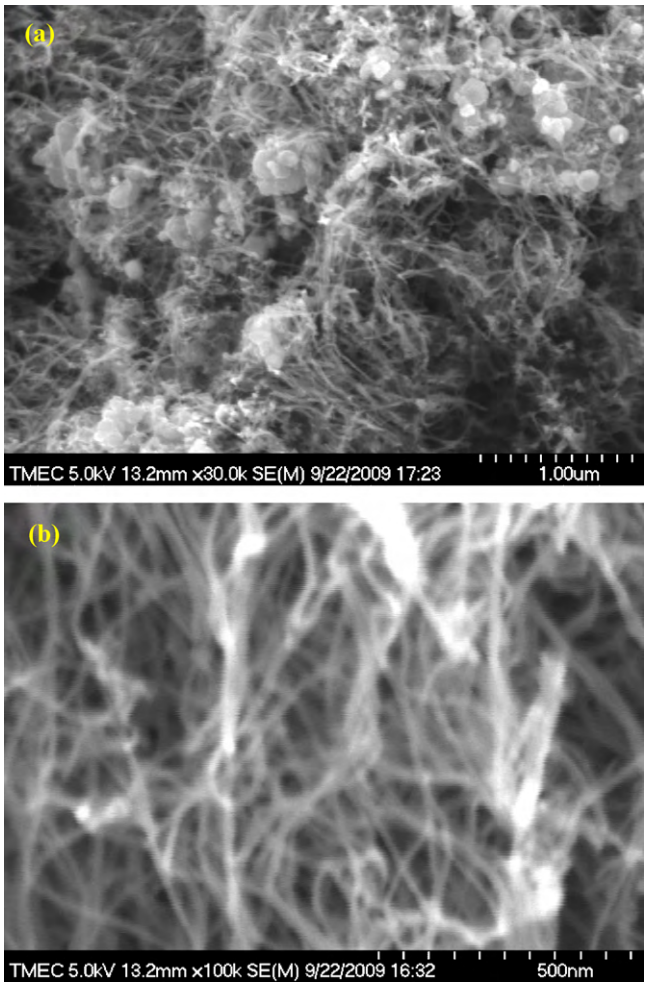

Fig. 2. SEM images of (a) a top view of CNTs on glass substrate with PVA and cholesterol enzyme coating and (b) a cross-sectional view of CNTs at high magnification.

al., 2004) while C–N bending band (740–800 cm^{-1}), COOH peak (1400 cm^{-1}), N–H bending peak (~1570 cm^{-1}: Amide II), C=O stretching peak (~1650 cm^{-1}: Amide I) as well as OH band can be attributed to enzyme molecules (Sulek et al., 2010).

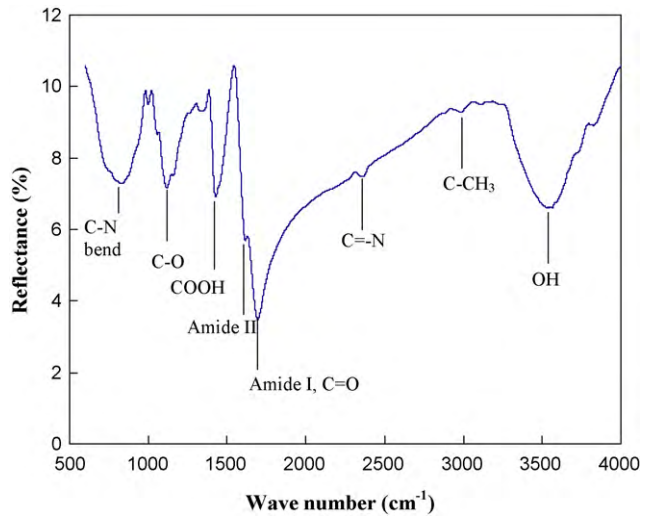

Fig. 3. Typical FTIR spectrum of the CNT electrode after PVA–cholesterol enzyme coating.

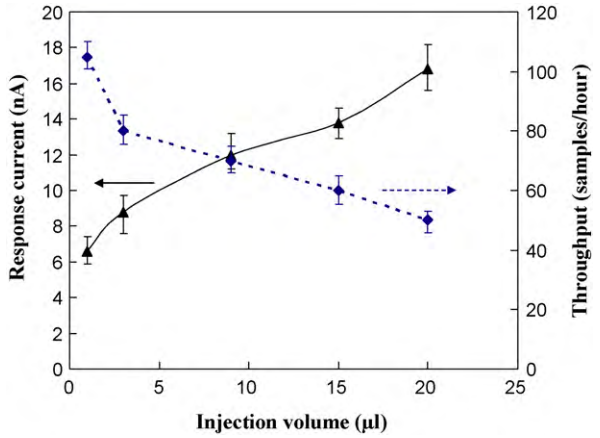

Fig. 4. Effect of injection volume on current response and sample throughput for cholesterol detection at 0.4 V vs. Ag reference electrode and 200 mg/dl cholesterol concentration.

3.2. Optimization of detection parameters

The detection potential affects the sensitivity as well as interference characteristics of current signal for bio-analytes. To obtain suitable detection potential, hydrodynamic voltammetry were studied from injection of 15 µl of 200 mg/dl cholesterol and acetaminophen solutions into the micro-flow system with varying detection potential from 0.3 to 0.7 V. It was found that signal to background (S/B) ratio gradually increased as potential increased from 0.3 to 0.7 V. However, interference from acetaminophen became significant at high detection potentials between 0.5 and 0.7 V. Therefore, 0.4 V bias potential was selected for cholesterol detection in all micro-flow experiments. If not indicated otherwise, sensors were prepared with cholesterol enzyme concentration of 75 U/ml and measurements were performed using PBS buffer with pH of 7 at room temperature (25 °C).

The influence of injection volume on the response of current signal and sample throughput was then characterized to optimize cholesterol detection. Fig. 4 shows current response and throughput vs. injection volume of 200 mg/dl cholesterol solution injected into the buffer stream flowed at a fixed rate at 40 µl/min. The throughput of detection is calculated from the total response time of injection. It can be seen that the current signal increases almost linearly while the throughput monotonically decreases with injection volume. The throughput decreases because the response time increases with injection volume. The injection volume of 15 µl was chosen for compromised sensitivity and throughput (60 samples/h). It should be noted that the *Y*-error bars in this plot (and all subsequent plots) represented the reproducibility from three sensors prepared in the same batch and measurement error over three repeated measurements. It can be seen that CNT sensors has good repeatability and reproducibility with relative standard deviations of less than 15%.

The effect of buffer pH on the sensor response was considered in the range between 6 and 8.5 using PBS buffer solutions. Fig. 5 shows the current response to 200 mg/dl cholesterol solution vs. buffer pH at a fixed buffer flow rate of 40 µl/min and a fixed sample injection volume of 15 µl. It is evident that the optimum pH is in the range between 7.0 and 7.5 and the response rapidly degrades under acidic and basic conditions. This is in accordance with other reports (Solanki et al., 2009; Umar et al., 2009) and the recommended pH for cholesterol oxidase (Noma and Nakayama, 1976). pH of 7 was selected to maximize the enzyme's life time.

The effect of enzyme concentration on the sensor response was studied in the range from 25 U/ml to 100 U/ml. Fig. 6 illustrates the current response to 200 mg/dl cholesterol solution as a func-

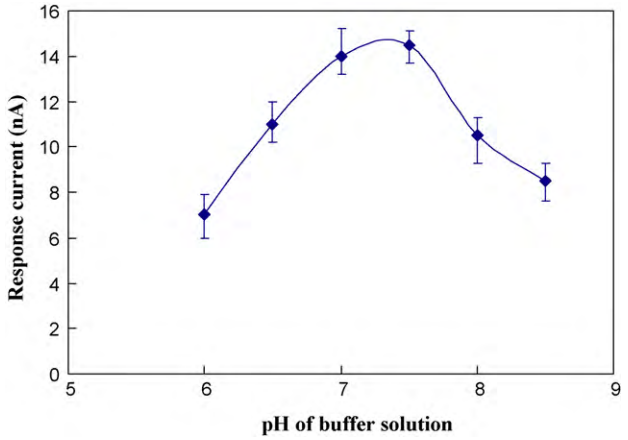

Fig. 5. Effect of buffer pH on current response to 200 mg/dl cholesterol at 0.4 V vs. Ag reference electrode.

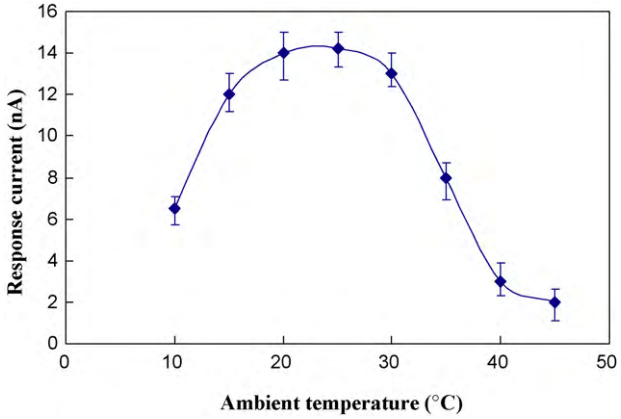

Fig. 7. Effect of ambient temperature on to 200 mg/dl cholesterol at 0.4 V vs. Ag reference electrode.

tion of enzyme concentration tested at a fixed buffer flow rate of 40 μl/min and a sample injection volume of 15 μl. It can be seen that the response initially increases as the enzyme concentration increases and then saturates when the concentration reaches 50 U/ml. Thus, the maximum enzyme entrapment was obtained at the enzyme concentration of 50 U/ml. However, enzyme concentration of 75 U/ml was used to ensure adequate enzyme loading for the remaining experiments.

The current response dependence on environmental temperature was investigated from 10 °C to 45 °C. Fig. 7 shows the current response to 200 mg/dl cholesterol solution vs. ambient temperature tested using a fixed buffer flow rate of 40 μl/min and a sample injection volume of 15 μl. It is evident that the current response is optimized in the temperature ranging from 20 to 30 °C. The response rapidly decreases when the ambient temperature exceeds 30 °C and it also reduces as temperature goes below 20 °C. The results can be explained from the fact that cholesterol enzyme quickly degrades at high temperature and electrochemical mobility and solubility of cholesterol in the solution reduce at low temperature. Thus, room temperature (25 °C) is suitable for cholesterol detection.

3.3. Amperometric detection of cholesterol

Amperometric cholesterol detection was then performed using the optimized detection potential, injection volume, pH of buffer, enzyme concentration and ambient temperature obtained from above studies. Fig. 8 shows amperometric cholesterol sensing in the concentration ranging from 50 to 250 mg/dl with three replicate injections for each concentration. From the plot, the rise time and decay time are estimated to be 3–5 and 40–45 s, respectively. Thus, fast detection with a high throughput of ~60 samples/h has been achieved.

The calibration curve, Fig. 9, is obtained from the peak amplitude of current response pulses over a range of concentration from 0 to 450 mg/dl. It can be seen that linear concentration dependence is obtained in the concentration range between 50 and 400 mg/dl (~1.25 to ~10 mM). The regression equation is given by $y = 0.0512x + 3.69$ ($r^2 = 0.9959$), where y and x are the height of peak current (nA) and cholesterol concentration (mg/dl), respectively. The slope of the equation is corresponding to the linear sensitivity of 0.0512 nA/(mg/dl). In addition, it is seen that the current response begins to level off at concentration higher than 400 mg/dl while it increases with a higher slope at concentration lower than 50 mg/dl. The detection limit (3S/N) is estimated from Fig. 9 to be ~10 mg/dl (~0.25 mM). Thus, the operating range of present system is suitable for clinical diagnostics of cholesterol in blood whose cholesterol concentration for most people lies within the range between 50 and 350 mg/dl.

The linear detection range is comparable to other electrochemical cholesterol sensors based on CNT nanocomposite or SnO_2/ZnO nanostructures (Li et al., 2005; Roy et al., 2006; Yang et al., 2006; Ansari et al., 2009; Solanki et al., 2009; Umar et al., 2009),

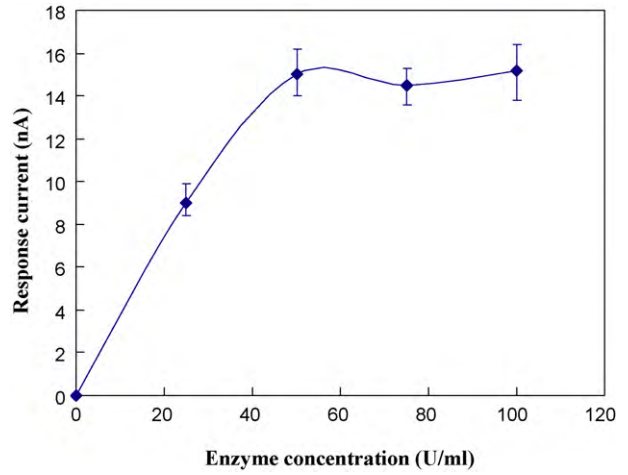

Fig. 6. Effect of cholesterol enzyme concentration on current response to 200 mg/dl cholesterol at 0.4 V vs. Ag reference electrode.

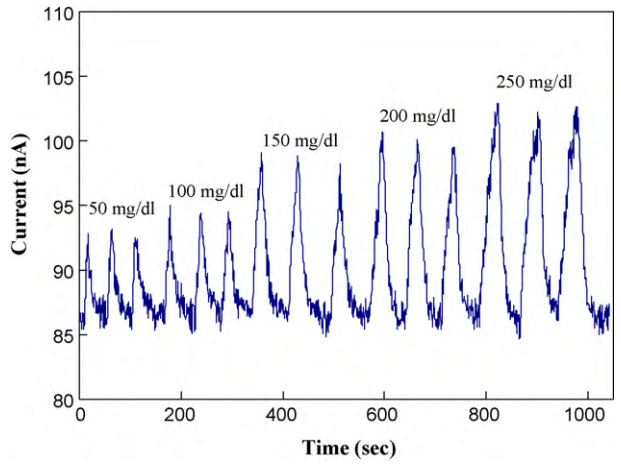

Fig. 8. Flow injection chronoamperometric detection of cholesterol with different cholesterol concentrations at 0.4 V vs. Ag reference electrode.

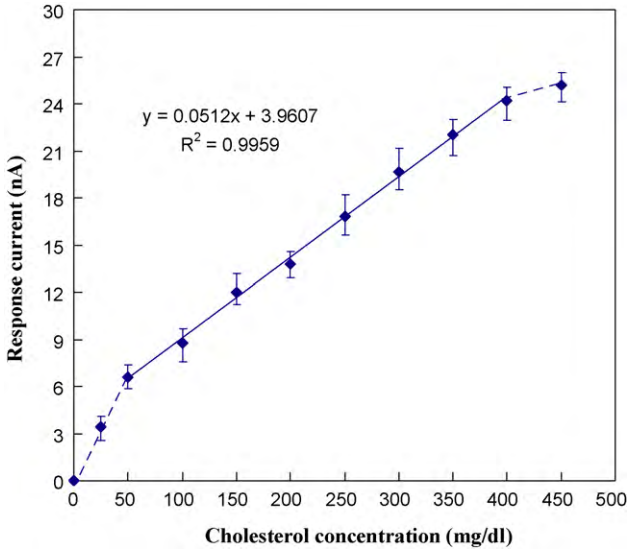

Fig. 9. Calibration curve as a function of cholesterol concentration.

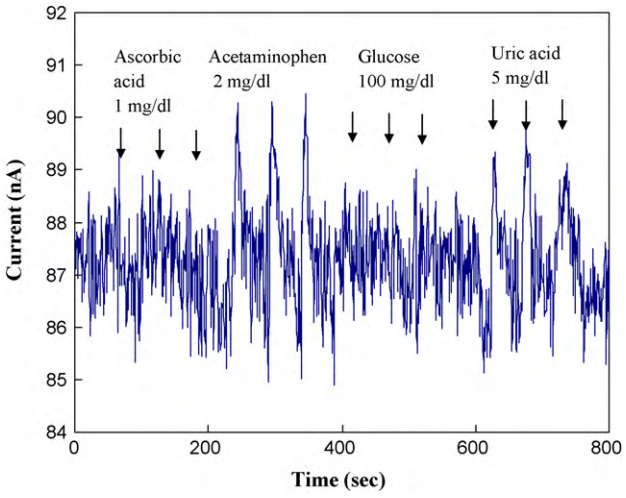

Fig. 10. Interference responses toward ascorbic acid (1 mg/dl), glucose (100 mg/dl), acetaminophen (2 mg/dl) and uric acid (5 mg/dl) at 0.4 V vs. Ag reference electrode.

whose linear regions are varied with high limits in the range of 300–500 mg/dl or 7.5–12.5 mM and with low limits in the range of 5–50 mg/dl or 0.1–1 mM. However, the detection limit is not as low as those in some reports, which are in the range of 0.05–5 mg/dl or 0.001–0.1 mM. The possible causes of relatively poor detection limit include less active enzymes used, less effective enzyme immobilization method and normally lower current sensitivity of micro-flow injection measurement.

It should be noted that this work utilizes dynamic micro-flow injection chronoamperometric detection scheme while other reports employ static/semi-static voltammetric detection methods including conventional chronoamperometry, cyclic voltammetry, square wave voltammetry and differential pulse voltammetry. In the micro-flow injection detection mode, sensors have very limited reaction time with very small sample volume and hence the response can be considerably less compared to other detection methods. Hence, the detection limit (10 mg/dl) and sensitivity (0.0512 nA/mg/dl) of the on-chip CNT sensor can be considered satisfactory and they may be comparable to other reported sensors if detection is made by the same method.

Despite its relatively lower current sensitivity, the proposed cholesterol detection scheme is considered better than several other reported cholesterol systems because of higher speed detection and much lower sample consumption. Real-time cholesterol detection has been achieved with very fast response time (3–5 s), high sample throughput (60 samples/h), very low sample consumption (15 μl) and satisfactory dynamic range (50–400 mg/dl). The resulting performance is attributed to fast, sensitive and stable CNT electrode directly grown on microfluidic chip and effective cholesterol enzyme immobilization using entrapment in PVA matrix. The use of this platform for other bio-sensing can be further optimized for each application by the use of suitable enzymes and immobilization methods to yield desired detection limit and dynamic range.

3.4. Interference and stability study

Specificity is one of the most critical issues for biosensors to be used in real environment. To evaluate specificity of the sensors, interferences by four common electroactive species including ascorbic acid, glucose, acetaminophen and uric acid were tested near their normal concentration level in serum. Fig. 10 demonstrates interference responses of ascorbic acid (1 mg/dl), glucose (100 mg/dl), acetaminophen (2 mg/dl) and uric acid (5 mg/dl). It can be seen that ascorbic acid and glucose give negligible interference signals, while acetaminophen and uric acid produce relatively small interference signal. The interferences from these analytes are satisfactorily low because the working electrode potential was set at a suitably low value of 0.4 V so that specific oxidative reaction by cholesterol oxidase is dominant.

Lastly, long-term stability of the sensor was assessed. The sensors were stored dry at 4 °C and tested every day. It was found that the sensitivity was dropped by 20% after one month due to natural enzyme degradation and loss during operation. No significant CNT removal was observed over the period of study. Thus, the on-chip CNT sensors had a satisfactory life time. The long-term stability of CNT electrode is attributed to the direct growth approach. The directly grown CNTs were robust to erosion under continuous flow of buffer and analyte for several days. Such stability may not be attained from CNTs prepared by paste printing or dielectrophoresis coating methods. Therefore, the present system is promising for clinical diagnostics of cholesterol with high speed real-time detection capability, very low sample consumption, high sensitivity, low interference and good stability.

4. Conclusions

In conclusion, a new cholesterol detection scheme utilizing functionalized CNT electrode on glass based microfluidic ship has successfully been developed by direct growth of CNTs on a glass chip. Fast cholesterol detection with a high throughput of more than 60 samples/h has been achieved. The CNTs based cholesterol sensor has a linear detection range between 50 and 400 mg/dl. In addition, low cross-sensitivity toward glucose, ascorbic acid, acetaminophen and uric acid have been verified. Moreover, the functionalized CNT electrode exhibits a good stability and good reproducibility in a micro-flow injection microfluidic system. The presented system is thus promising for clinical diagnostics of cholesterol with high speed real-time detection capability, very low sample consumption, high sensitivity, low interference and good stability.

Acknowledgements

This work was supported by National Electronics and Computer Technology Center (NECTEC), project no. ME5101, and Thailand

Research Fund (TRF). A.T. would like to acknowledge TRF for career developing fund.

References

Ansari, A.A., Kaushik, A., Solanki, P.R., Malhotra, B.D., 2009. Electroanalysis 21, 965–972.
Ansari, A.A., Kaushik, A., Solanki, P.R., Malhotra, B.D., 2008. Electrochem. Commun. 10, 1246–1249.
Aravamudhan, S., Kumar, A., Mohapatra, S., Bhansali, S., 2007. Biosens. Bioelectron. 23, 2289–2294.
Arya, S.K., Pandey, P., Singh, S.P., Datta, M., Malhotra, B.D., 2007. Analyst 132, 1005–1009.
Arya, S.K., Datta, M., Malhotra, B.D., 2008. Biosens. Bioelectron. 23, 1083–1100.
Becker, H., Locascio, L.E., 2002. Talanta 56, 267–287.
Brahim, S., Narinesingh, D., Elie, A.G., 2002. Biosens. Bioelectron. 17, 973–981.
Castano-Alvarez, M., Fernansez-Abedul, M.T., Costa-Garcia, A., 2006. J. Chromatogr. A 1109, 291–299.
Crevillen, A.G., Pumera, M., Gonzalez, C.M., Escarpa, A., 2009. Lab Chip 9, 346–353.
Dossi, N., Susmel, S., Toniolo, R., Pizzariello, A., Bontempelli, G., 2009. Electrophoresis 30, 3465–3471.
Dossi, N., Toniolo, R., Pizzariwllo, A., Susmel, S., Perennes, F., Bontempelli, G.J., 2007. Electroanal. Chem. 601, 1–7.
Ford, S.M., Kar, B., McWhorter, S., Davies, J., Soper, S.A., Klopf, M., Calderon, G., Saile, V.J., 1998. Microcolumn 10, 413–422.
Guo, M., Chen, J., Li, J., Nie, L., Yao, S., 2004. Electroanalysis 16, 1992–1998.
Huang, J.-E., Hong, X., Li, H.-L., 2003. Carbon 41, 2731–2736.
Karuwan, C., Wisitsoraat, A., Maturos, T., Phokharatkul, D., Sappat, A., Jaruwongrungsee, K., Lomas, T., Tuantranont, A., 2009. Talanta 79, 995–1000.
Kaushik, A., Solanki, P.R., Kaneto, K., Kim, C.G., Ahmad, S., Malhotra, B.D., 2010. Electroanalysis 22, 1045–1055.
Kirgoz, U.A., Timur, S., Odaci, D., Pérez, B., Alegret, S., Merkoçi, A., 2007. Electroanalysis 19, 893–899.
Li, J., Peng, T., Peng, Y., 2003. Electroanalysis 15, 1031–1037.
Li, G., Liao, J.M., Hu, G.Q., Ma, N.Z., Wu, P.J., 2005. Biosens. Bioelectron. 20, 2140–2144.
Li, Y., Bai, H., Liu, Q., Bao, J., Han, M., Dai, Z., 2010. Biosens. Bioelectron. 25, 2356–2360.
Liao, K.-T., Chen, C.-M., Huang, H.-J., Lina, C.-H., 2007. J. Chromatogr. A 1165, 213–218.
Lin, K.-W., Huang, Y.-K., Su, H.-L., Hsieh, Y.-Z., 2008. Anal. Chim. Acta 619, 115–121.
Mansur, H.S., Orefice, R.L., Mansur, A.A.P., 2004. Polymer 45, 7193–7202.
McDonald, J.C., Duffy, D.C., Anderson, J.R., Chiu, D.T., Wu, H., Schueller, O.J.A., Whitesides, G.M., 2000. Electrophoresis 21, 27–40.
Noma, A., Nakayama, K., 1976. Clin. Chem. 22, 336.
Panini, N.V., Messina, G.A., Salinas, E., Fernandez, H., Raba, J., 2008. Biosens. Bioelectron. 20, 2140–2144.
Pozo-Ayuso, D.F., Castano-Alvarez, M., Fernansez-la-Villa, A., Garcia-Granda, M., Fernandez-Abedul, M.T., Costa-Garcia, A., Rodriguez-Garcia, J., 2008. J. Chromatogr. A 1180, 193–202.
Qiaocui, S., Tuzhi, P., Yunu, Z., Yang, C.F., 2005. Electroanalysis 17, 857–861.
Roy, S., Vedala, H., Choi, W., 2006. Nanotechnology 17, S14–S18.
Rwyes, D.R., Iossifidis, D., Auroux, P.A., Manz, A., 2002. Anal. Chem. 74, 2623–2636.
Schoning, M.J., Jacobs, M., Muck, A., Knobbe, D.-T., Wang, J., Chatrathi, M., Spillmamm, S., 2005. Sens. Actuators B 108, 688–694.
Shahrokhian, S., Zare-Mehrjardi, H.R., 2007. Electrochim. Acta 52, 6310–6317.
Solanki, P.R., Kaushik, A., Ansari, A.A., Tiwari, A., Malhotra, B.D., 2009. Sens. Actuators B 137, 727–735.
Sulek, F., Knez, Z., Habulin, M., 2010. Appl. Surf. Sci. 256, 4596–4600.
Umar, A., Rahman, M.M., Al-Hajry, A., Hahn, Y.-B., 2009. Talanta 78, 284–289.
Vidal, J.C., Ruiz, E.G., Castillo, J.R., 2001. Electroanalysis 13, 229–235.
Wisitsoraat, A., Tuantranont, A., Thanachayanont, C., Patthanasettakul, V., Singjai, P., 2006. J. Electroceram. 17, 45–49.
Wisitsoraat, A., Patthanasettakul, V., Tuantranont, A., Mongpraneet, S., 2008. J. Vac. Sci. Technol. B 26, 1757–1760.
Wisitsoraat, A., Karuwan, C., Wong-ek, K., Phokharatkul, D., Phokharatkul, P., Tuantranont, A., 2009. Sensors 9, 8658–8668.
Yang, M., Yang, Y., Qu, F., Lu, Y., Shen, G., Yu, R., 2006. Anal. Chim. Acta 571, 211–217.

Please cite this article in press as: Wisitsoraat, A., et al., Biosens. Bioelectron. (2010), doi:10.1016/j.bios.2010.07.101